Basic Res Cardiol (2012) 107:244
DOI 10.1007/s00395-012-0244-x

ORIGINAL CONTRIBUTION

# Cell-to-cell variability in troponin I phosphorylation in a porcine model of pacing-induced heart failure

**Dániel Czuriga · Attila Tóth · Enikő T. Pásztor · Ágnes Balogh · Andrea Bodnár · Enikő Nizsalóczki · Vincenzo Lionetti · Fabio A. Recchia · István Czuriga · István Édes · Zoltán Papp**

Received: 4 December 2011 / Revised: 12 December 2011 / Accepted: 31 December 2011 / Published online: 12 January 2012


**Abstract** We tested the hypothesis that myocardial contractile protein phosphorylation and the $Ca^{2+}$ sensitivity of force production are dysregulated in a porcine model of pacing-induced heart failure (HF). The level of protein kinase A (PKA)-dependent cardiac troponin I (TnI) phosphorylation was lower in the myocardium surrounding the pacing electrode (pacing site) of the failing left ventricle (LV) than in the controls. Immunohistochemical assays of the LV pacing site pointed to isolated clusters of cardiomyocytes exhibiting a reduced level of phosphorylated TnI. Flow cytometry on isolated and permeabilized cardiomyocytes revealed a significantly larger cell-to-cell variation in the level of TnI phosphorylation of the LV pacing site than in the opposite region in HF or in either region in the controls: the interquartile range (IQR) on the distribution histogram of relative TnI phosphorylation was wider at the pacing site (IQR = 0.53) than that at the remote site of HF (IQR = 0.42; $P = 0.0047$) or that of the free wall of the control animals (IQR = 0.36; $P = 0.0093$). Additionally, the $Ca^{2+}$ sensitivities of isometric force production were higher and appeared to be more variable in single permeabilized cardiomyocytes from the HF pacing site than in the healthy myocardium. In conclusion, the level of PKA-dependent TnI phosphorylation and the $Ca^{2+}$ sensitivity of force production exhibited a high cell-to-cell variability at the LV pacing site, possibly explaining the abnormalities of the regional myocardial contractile function in a porcine model of pacing-induced HF.

**Keywords** Cardiac function · Pacing-induced heart failure · $\beta$-adrenergic signaling · Dilated cardiomyopathy · Cardiac troponin I

**Electronic supplementary material** The online version of this article (doi:10.1007/s00395-012-0244-x) contains supplementary material, which is available to authorized users.

D. Czuriga · A. Tóth · E. T. Pásztor · Á. Balogh · I. Czuriga · I. Édes · Z. Papp (✉)
Division of Clinical Physiology, Research Center for Molecular Medicine, Institute of Cardiology, Faculty of Medicine, University of Debrecen, Medical and Health Science Center, Móricz Zs. krt. 22, 4032 Debrecen, Hungary
e-mail: pappz@med.unideb.hu

A. Bodnár · E. Nizsalóczki
HAS-UD Cell Biology and Signaling Research Group, Department of Biophysics and Cell Biology, University of Debrecen, Medical and Health Science Center, Debrecen, Hungary

V. Lionetti · F. A. Recchia
Sector of Medicine, Scuola Superiore Sant'Anna, Pisa, Italy

V. Lionetti · F. A. Recchia
Fondazione CNR-Regione Toscana "G. Monasterio", Pisa, Italy

F. A. Recchia
Department of Physiology, New York Medical College, Valhalla, NY, USA

## Introduction

Changes in the expression and post-translational modifications of myocardial proteins occur in the molecular background of myocardial remodeling during the development of chronic heart failure (HF). These alterations affect the myocardial structure and are responsible for disturbances in cellular functions ranging from intracellular signaling through cardiomyocyte contractility to metabolism. In this context, a number of studies have implicated the involvement of myofilamentary proteins in the progressive decay of the myocardial function [12, 30, 33, 42]. In the failing human heart, a downgraded $\beta$-adrenergic

responsiveness was found to be associated with an increased $Ca^{2+}$ sensitivity of force production through a diminished level of protein kinase A (PKA)-mediated troponin I (TnI) and myosin-binding protein-C (MyBP-C) phosphorylation [6, 27, 41, 43–45], although these relationships were not fully confirmed in all models of HF [4, 5, 28, 37]. Some of the discrepancies arise from the complexity of the human pathology, the difficulty of finding reliable human control materials, and possible species-dependent differences between signaling pathways in large and small mammals [26, 35]. It follows that investigations in large animal models of HF are of great importance, as they will possibly elucidate HF-specific protein alterations with direct relevance for the human pathology.

A well-established large animal model of HF, induced by continuous cardiac pacing at a frequency three- to fourfold higher than the spontaneous heart rate, is mostly applied to dogs, pigs, sheep, and monkeys [15, 34]. One characteristic of this model is the presence of regional differences in functional and molecular remodeling. For example, in a canine tachy-pacing HF model, regional differences were noted in the extent of action potential prolongation and intracellular $Ca^{2+}$ homeostasis abnormalities [1]. Moreover, cardiac resynchronization therapy in these hearts furnished non-uniform responses [2]. In a porcine model of HF, sustained pacing-induced dyssynchronous left ventricular (LV) activation caused more pronounced decreases in LV systolic thickening and circumferential shortening in the anterior/anterolateral region (pacing site) as compared with the inferoseptal region (opposite site) (to $\sim 7$ vs. $\sim 31\%$ and to $\sim -5$ vs. $\sim -7\%$, respectively), which were unrelated to a uniform increase in glucose uptake in the corresponding regions [further parameters of in vivo hemodynamic alterations of this model have been detailed in a previous study [23] (p. H2750, Table 1)]. However, these changes did correlate with an asymmetrical myocardial expression of natriuretic peptides [10].

In the present study, we set out to investigate a hypothetical relationship between PKA-dependent myofilament hypophosphorylation and the contractile dysfunction in a porcine model of pacing-induced HF. With a view to analyzing PKA-dependent TnI phosphorylation at the tissue and cellular levels, we performed biochemical studies (back-phosphorylation) in tissue homogenates, immunohistochemical studies in LV tissue slices, and flow cytometric assays in a large number of permeabilized cardiomyocytes isolated from paced and non-paced regions of failing LVs. To assess functional correlates, we measured the $Ca^{2+}$ sensitivity of isometric force production ($pCa_{50}$) and additional mechanical parameters of isolated cardiomyocytes of failing and healthy hearts.

Our data revealed disparate myocardial tissue characteristics within the LV of the HF animals and hence suggested a plausible explanation for the dyssynchronous LV activation.

## Materials and methods

### Experimental tissue material

Ten male, sexually mature minipigs (35–40 kg) were chronically instrumented in the laboratory of the Sector of Medicine, Scuola Superiore Sant'Anna, Pisa, Italy. HF was induced by pacing the LV anterior wall at 180 beats/min for 3 weeks. Pigs were considered to develop severe HF when the LV end-diastolic pressure was $\geq$20 mmHg and the ejection fraction was <40%. Untreated animals were used as healthy controls. Hemodynamic measurements, MRI and PET examinations were performed in controls and in HF animals and identified regional wall motion abnormalities as reported earlier [23]. The minipigs were then killed and their hearts were removed, dissected, and immediately frozen in liquid nitrogen. The anterolateral

**Table 1** Descriptive values for the distribution histograms of the flow cytometric experiments

| [log(P-TnI/TnI)] distribution | Control pacing site ($n = 6$) | Control opposite site ($n = 6$) | HF pacing site ($n = 6$) | HF opposite site ($n = 6$) |
|---|---|---|---|---|
| 25% percentile | *−0.45* | *−0.46* | *−0.65* | *−0.57* |
| Median | *−0.27* | *−0.26* | *−0.37* | *−0.36* |
| 75% percentile | *−0.09* | *−0.09* | *−0.12* | *−0.15* |
| IQR | 0.36 | 0.37 | $0.53^{+,\#}$ | 0.42 |
| Mean | −0.28 | −0.29 | −0.41* | −0.38 |
| Std. deviation | *0.29* | *0.31* | *0.43* | *0.35* |
| Std. error of mean | *0.002* | *0.002* | *0.003* | *0.002* |

Rows in italics were not analyzed statistically since these parameters cannot be interpreted at the single-particle level

* $P = 0.0071$ HF pacing versus control pacing site

$^{+}$ $P = 0.0093$ HF pacing versus control pacing site

$^{\#}$ $P = 0.0047$ HF pacing versus HF opposite site

wall (pacing site) and inferoseptal region (opposite site) of the LVs were separated. Transfer of the cardiac samples between laboratories was performed on dry ice. The pigs were treated and housed in accordance with the Italian national guidelines (No. DLGS 27/01/1992, No. 116).

### Immunohistochemistry

Porcine heart samples were sectioned in a cryostat at −20°C to obtain 10-μm-thick slices. All subsequent steps were performed at room temperature. Slides were fixed with ice-cold acetone for 5 min and incubated in methanol for 20 min. The fixed slides were then rinsed in PBS (containing 150.7 mM NaCl, 3.22 mM KCl, 0.735 mM $KH_2PO_4$, 8.6 mM $Na_2HPO_4$; pH 7.4) and blocked for 20 min in normal goat serum. A monoclonal mouse anti-TnI primary antibody (Clone 19C7, Research Diagnostics Inc., Flanders, USA; 1:500 dilution in PBS-BSA) was used to analyze TnI independently of its phosphorylation status, and a polyclonal rabbit anti-TnI (phospho S22 + S23) (Abcam, Cambridge, UK; 1:500 dilution in PBS-BSA) was employed to assess PKA-mediated TnI phosphorylation (P-TnI). Slides were incubated overnight at +4°C, followed by a 30-min incubation at room temperature with anti-mouse-Cy3 (red) and anti-rabbit-Cy2 (green) antibodies (Jackson Laboratories, Bar Harbor, ME, USA; 1:200 dilution in PBS) to visualize cardiac TnI and its PKA-specific phosphorylated form. To assess protein kinase C (PKC)-mediated TnI phosphorylation, polyclonal rabbit anti-TnI primary antibody (phospho T143) (Abcam, Cambridge, UK; 1:100 dilution in PBS-BSA) was used, followed by overnight incubation at +4°C, then 30 min incubation at room temperature with anti-rabbit-Biotin antibody (Jackson Laboratories, Bar Harbor, ME, USA; dilution: 1:200). Streptavidin-Cy2 (green) was used to visualize PKC-specific phosphorylation of TnI. Microscope slides were mounted with Vectashield mounting medium containing 4′,6-diamidino-2-phenylindole (DAPI) (Vector Laboratories, Burlingame, CA, USA). Microscopic images of tissue cuts were recorded with a NIKON Eclipse 80i Fluorescein microscope, using a NIKON 10× objective (NA:0.30) at 100× magnification. High-quality images were recorded with an Olympus FluoView 1000 Confocal microscope, using an Olympus LUCPLFLN 20× objective (NA:0.45) and digital zoom at 180× and 540× magnifications.

### Back-phosphorylation of TnI

A back-phosphorylation assay was performed to assess the phosphorylation level of TnI in protein homogenates of permeabilized cardiomyocytes [11]. Permeabilized cardiomyocytes were prepared as described elsewhere [8]. Reaction mixtures contained 40 μl of the isolated cardiomyocyte fraction {protein concentration 0.5 mg/ml in a modified isolation solution [in mM: KCl 100, ethylene glycol tetra-acetic acid (EGTA) 2, $MgCl_2$ 1, ATP 0.1, and imidazole 100; pH 7.0; all chemicals from Sigma-Aldrich, St. Louis, MO, USA]}, 10 μl of modified isolation solution containing $^{32}$P-labeled ATP (final specific activity: 1,500 cpm/pmol), and 1 μl of PKA [from Sigma, St. Louis, MO, USA, 4,000 U/ml in 6 mg/ml of (dithiothreitol) DTT-containing modified isolation solution]. The reaction was performed at room temperature for 15 min. At the end, 50 μl of sodium dodecyl sulfate (SDS) sample buffer (Sigma-Aldrich, St. Louis, MO, USA) was added and the samples were boiled for 5 min. Thirty microliters of boiled samples was loaded onto 10% polyacrylamide gels, separated, and transferred onto nitrocellulose membranes. Phosphate incorporation into TnI was detected by autoradiography (blue-sensitive RTGB films from Primax, Berlin, Germany). Band intensities (reflecting phosphate incorporation) were determined by densitometry using Image J software (freeware from http://www.nih.gov). Optical densities are shown in arbitrary units in the Figures.

### Western immunoblotting

Porcine LV tissue samples were homogenized in radioimmune precipitation assay buffer containing Tris–Cl 50 mM, NaCl 150 mM, 1% Triton X-100, 0.1% SDS, and 1% sodiumdeoxycholate; pH 7.4. Protein concentrations were determined by BCA assay (Sigma-Aldrich, St. Louis, MO, USA) using bovine serum albumin (BSA) as standard, and the concentration of each homogenate was adjusted to 4 mg/ml. The homogenates were then mixed with an equal volume of 2× SDS sample buffer (Sigma-Aldrich, St. Louis, MO, USA) and were boiled for 10 min before electrophoresis. 50 μg of proteins was loaded onto 10% SDS-polyacrylamide gels and, after separation, transferred to nitrocellulose membranes. The membranes were probed with antibodies against TnI (Clone 19C7, Research Diagnostics Inc., Flanders, NJ, USA, dilution: 1:5,000) and the signal was detected with a peroxidase-conjugated anti-rabbit IgG-specific antibody (Sigma-Aldrich, St. Louis, MO, USA; dilution: 1:50,000). The bands were visualized by enhanced chemiluminescence and evaluated with Image J software. Only bands on the same membrane were used to avoid alterations due to differences in transfer efficiency or other technical reasons.

### Flow cytometry

LV tissue samples (∼0.04 g wet weight) were mechanically disrupted and isolated as described earlier. In brief, the isolated cells were permeabilized in cell isolation solution (in mM: $MgCl_2$ 1, KCl 100, EGTA 2, ATP 4, and

imidazole 10; pH 7.0; all chemicals from Sigma-Aldrich, St. Louis, MO, USA) as described elsewhere [29]. Thereafter, the myocytes were incubated on ice for 90 min in 100 µl of isolation solution containing 2 mg/ml BSA (Sigma-Aldrich, St. Louis, MO, USA) and primary antibody. Monoclonal mouse anti-TnI antibody (Clone 19C7, Research Diagnostics Inc., Flanders, NJ, USA; dilution: 1:200), and a phosphorylation-sensitive polyclonal rabbit anti-TnI antibody (phospho S22 + S23) (Abcam, Cambridge, UK; 1:100 dilution) were used as primary antibodies, followed by a 30-min incubation on ice with anti-mouse-Cy3 and anti-rabbit-Cy5 antibodies (Jackson Laboratories, Bar Harbor, ME, USA; dilution: 1:50) to label cardiac TnI and P-TnI. Myocytes were fixed with ice-cold 2% formaldehyde solution (in cell isolation solution) for 30 min. All washing steps were performed with isolation solution. The cell suspensions were gently sonicated and then filtered through a 50-µm-wide cell filter. Flow cytometric experiments were carried out on a FACSArray flow cytometer (Becton–Dickinson, San Jose, CA, USA). Fluorescence intensities for single particles were determined in six animals per group. 6,000–10,000 particles were measured per animal. Cy3 fluorescence was excited at 532 nm and detected at 585 ± 21 nm, whereas Cy5 was excited at 635 nm and detected at 661 ± 8 nm. Cell debris was excluded from the analysis by gating on the forward and right angle light scatter signals. List mode files were analyzed with the software REFLEX [39].

## Force measurements in permeabilized cardiomyocyte preparations

The force at saturating [$Ca^{2+}$] ($F_o$), the passive force component ($F_{passive}$), the $Ca^{2+}$ sensitivity of isometric force production ($pCa_{50}$), the steepness of the $Ca^{2+}$–force relationship ($n_{Hill}$), and the rate constant of force redevelopment at saturating $Ca^{2+}$ levels ($k_{tr,max}$; specific for the maximal turnover rate of the actin-myosin cross-bridge cycle) were used as parameters of the myofibrillar function. Moreover, these mechanical data were determined at sarcomere lengths (SLs) of 1.9 and 2.3 µm to test for possible alterations in length-dependent $Ca^{2+}$ sensitization, i.e. in the molecular background of the Frank-Starling mechanism. The pCa, i.e. $-\log[Ca^{2+}]$, values of the relaxing solution and the activating solution used during the force measurements (pH 7.2) were 9.0 and 4.75, respectively. The composition of the relaxing solution differed from that of the activating solution only in the use of 7 mM EGTA instead of Ca-EGTA. Both solutions were supplemented with protease inhibitors: 0.5 mM phenylmethylsulfonyl fluoride (PMSF) (Sigma-Aldrich, St. Louis, MO, USA), 40 µM leupeptin (Sigma-Aldrich, St. Louis, MO, USA), and 10 µM E-64 (Sigma-Aldrich, St. Louis, MO, USA).

The technique employed for force measurements in a single myocyte-sized preparation was detailed earlier [29]. Briefly, a single permeabilized cardiomyocyte was attached to a mechanical measuring system. After precise SL adjustment to 2.3 µm, isometric $Ca^{2+}$ contractures were evoked at 15°C during repeated activation–relaxation cycles by moving the myocyte from $Ca^{2+}$-free relaxing solution to activating solutions of gradually increasing [$Ca^{2+}$]. Isometric force values were normalized for maximal $Ca^{2+}$-activated active force, and $Ca^{2+}$–force relations were plotted and fitted with a modified Hill function to determine the $Ca^{2+}$ sensitivity of isometric force production, i.e. $pCa_{50}$, and the cooperativity within the contractile machinery ($n_{Hill}$). $Ca^{2+}$–force relationships were determined before and after in vitro PKA exposures. The PKA stock solution contained the catalytic subunit of PKA from bovine heart [100 U in distilled water supplemented with 6 mg/ml of DTT at a protein concentration of 0.05 mg/ml, as recommended by the manufacturer (Sigma-Aldrich, St. Louis, MO, USA; Catalog number: P2645; LOT number: 021M7676V)]. To assess the effects of PKA, cardiomyocytes were incubated for 20 min in 100 µl of relaxing solution supplemented with 5 µl of the PKA stock solution. In a separate study, isometric force measurements were performed first at a SL of 1.9 µm and then at a SL of 2.3 µm.

During single $Ca^{2+}$ contractures, once the peak force was reached, the rate constant of force redevelopment ($k_{tr,max}$) was determined by a quick release–restretch maneuver in the activating solution. As a result of this intervention, the force dropped from peak level to zero, allowing determination of the total force level ($F_{total}$), and then started to redevelop. The cardiomyocyte was next returned to the relaxing solution, where a shortening to 80% of the original preparation length was performed to assess the passive force level ($F_{passive}$). The active isometric force ($F_o$) was calculated by subtracting the passive force from the total isometric force. $F_o$ and $F_{passive}$ were normalized for the cardiomyocyte cross-sectional area, calculated from the width and thickness of the myocyte, which were measured with optically directed light.

## Data analysis, statistics

$Ca^{2+}$–force relations were fitted to a modified Hill equation:

$$F = F_o\left[Ca^{2+}\right]^{n_{Hill}} / \left(Ca_{50}^{n_{Hill}} + \left[Ca^{2+}\right]^{n_{Hill}}\right)$$

where $F$ is the steady-state force at a given [$Ca^{2+}$], while $F_o$, $n_{Hill}$ and $Ca_{50}$ (or $pCa_{50}$) denote the maximal $Ca^{2+}$-activated force at saturating [$Ca^{2+}$], and the slope and midpoint of the sigmoidal relationship, respectively.

The force redevelopment after the release–restretch maneuver was fitted to a single exponential function in

order to estimate the rate constant of force redevelopment ($k_{tr,max}$) at the maximal [$Ca^{2+}$] level:

$$F(t) = F_i + F_a\left(1 - e^{-k_{tr,max}t}\right)$$

where $F(t)$ is the force at any time ($t$) after the restretch at the maximal [$Ca^{2+}$], and $F_i$ and $F_a$ denote the initial force after the restretch and the amplitude of $Ca^{2+}$-activated force redevelopment, respectively. Each experimental preparation was fitted individually, the fitted parameters were pooled, and the mean values are reported.

Statistical analyses of the back-phosphorylation assay and mechanical measurements were performed by ANOVA followed by a Bonferroni test for multiple comparisons between groups. Relationships between two continuous variables were assessed with linear regression analysis. Differences due to PKA treatment during mechanical measurements were analyzed using a paired Student's $t$ test. Statistical significance was accepted at $P < 0.05$. Analysis of the thousands of single data points obtained from the flow cytometric measurements required a modeling method that does not assume independence across single particles, but is able to handle the correlation between particle-level measurements within the same animal's heart. Thus, conventional ANOVA or linear regression could not be used, but maximum likelihood mixed effects multilevel modeling with interaction between groups and sites was found to be appropriate. Estimation of the pacing effect was based on mean log relative signal intensities [log(P-TnI/TnI)] for the level of phosphorylation and on interquartile ranges (IQRs) for the heterogeneity of phosphorylation. Logarithmic transformation of the data improved the normality of the distribution of the variables.

## Results

To test homogeneity in PKA-mediated myofilament protein phosphorylation, the level of TnI phosphorylation was visualized during immunohistochemical studies on myocardial tissue samples in the anterior/anterolateral (pacing site) and in the inferoseptal regions (opposite site) in HF and control hearts. Myocardial tissue samples were labeled with specific antibodies against TnI, the phosphorylated form of TnI (P-TnI) at PKA-specific sites (S22 + S23), and slides were also mounted with DAPI-containing medium. In Fig. 1, beside the three separate signals captured with fluorescent light microscopy, merged pictures from each group are also shown. In general, the staining of tissue slices for P-TnI resulted in a more homogeneous staining intensity in the controls and opposite site of HF hearts than in the pacing site of HF hearts, where areas with various P-TnI intensity levels could be observed. Areas with given staining intensities were formed by clusters of cardiomyocytes with similar P-TnI signal levels in the pacing site of HF hearts (Fig. 1b). The P-TnI staining did not appear to vary within single cardiomyocytes. The homogenous picture with phosphorylation-insensitive TnI antibody and the identification of cardiomyocyte nuclei by DAPI were in contrast with the inhomogeneous pattern observed following P-TnI staining in the same myocardial sections, and hence indicated that fibrosis or necrosis could not explain the heterogeneous staining pattern at the pacing sites of HF hearts. In a separate study, we also attempted to test the homogeneity of PKC-mediated TnI phosphorylation at the pacing site of HF animals. To this end, myocardial tissue samples were labeled similarly as those in Fig. 1 for the PKA-specific TnI phosphorylation sites and also with antibodies specific for a PKC-specific TnI phosphorylation site (T143) (Online Resource 1). In general, these sections suggested TnI phosphorylation to be more homogenous at the PKC site than at the PKA-specific sites.

The mean levels of myofilament protein phosphorylation were tested in a back-phosphorylation assay. The mean phospho-specific TnI signal intensity of protein homogenates of permeabilized cardiomyocytes from the pacing sites of the HF animals (58 ± 14.49 AU) was significantly higher than that in the control pigs (5.41 ± 1.34 AU; $P < 0.05$), which was suggestive of a PKA-dependent phosphorylation deficit of TnI at the HF pacing site (Fig. 2a, b). The phosphorylation-dependent intensities at the molecular masses of 20 and 150 kDa [i.e. close to those of MyBP-C and myosin light chain 2 (MLC2)] correlated with TnI phosphorylation (Fig. 2c). Parallel changes in TnI phosphorylation and MyBP-C phosphorylation are expected upon PKA applications; however, phosphate incorporation into MLC2 is not expected for PKA exposures, and hence the protein at 20 kDa could be a protein other than MLC2. The difference in the overall phosphorylation level of myocardial TnI (P-TnI) between the pacing and the opposite sites of the HF pigs did not reach significance ($P > 0.05$) (HF opposite site: 40.3 ± 9.86 AU) (Fig. 2a, b).

Motivated by the results of our histochemical observations and back-phosphorylation assays, we developed a protocol that allowed the quantitative evaluation of regional differences in the level of TnI phosphorylation in suspensions of permeabilized cardiomyocytes by flow cytometry. This method yielded relative P-TnI levels in a vast number of cardiomyocytes following dual-labeling of cardiomyocytes for TnI and P-TnI (Fig. 3a). Distribution histograms of logarithmically transformed relative signal intensities [log(P-TnI/TnI)] were then expressed for the two regions of interest in the HF and control groups by pooling data from six hearts in each group. Figure 3b shows that the distribution histogram of the pacing site in the controls demonstrated close to Gaussian distribution, in

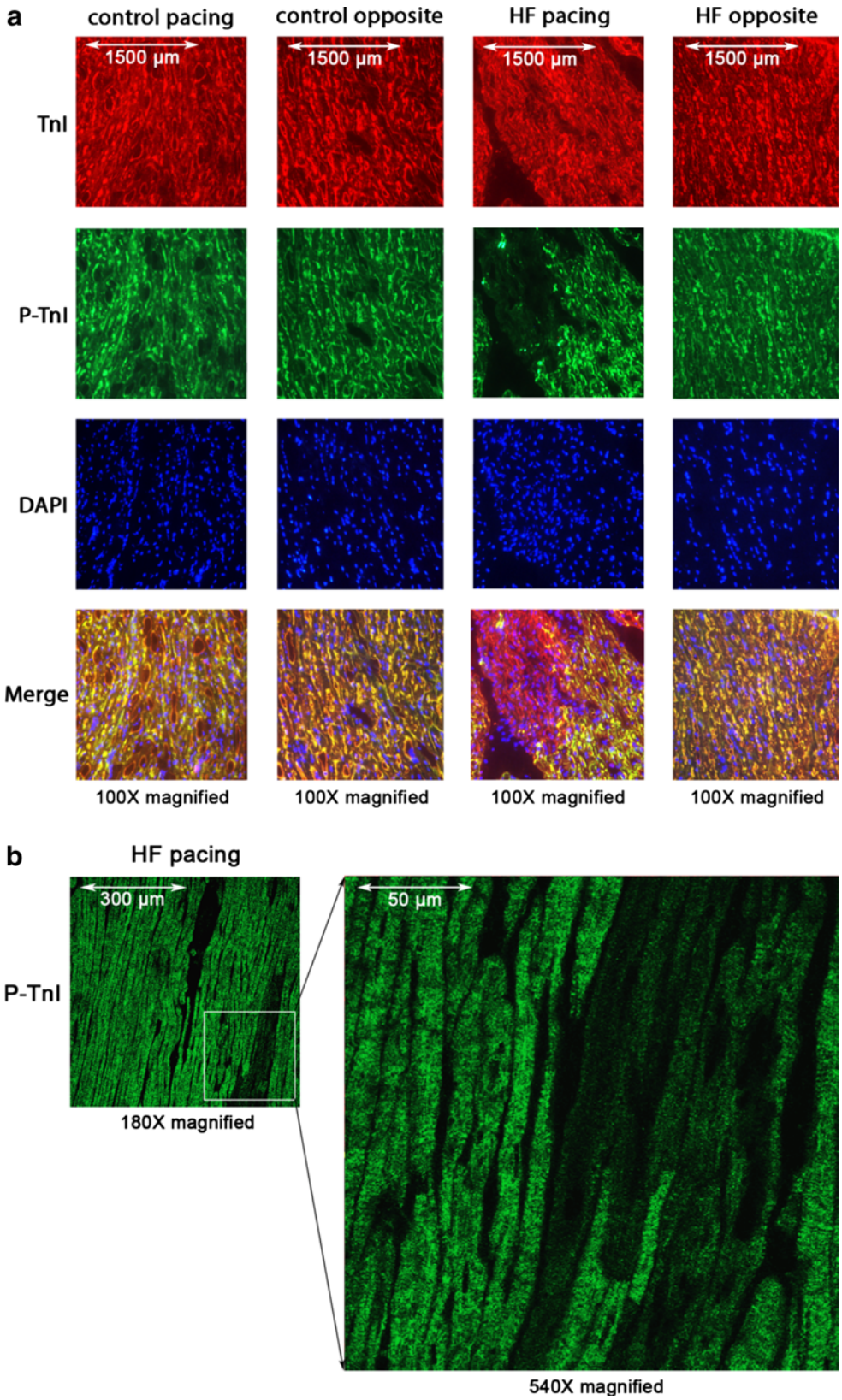


**Fig. 1** Immunohistochemistry. **a** Myocardial tissue samples were labeled with specific antibodies against TnI, the phosphorylated form of TnI (P-TnI) and nuclei with DAPI. Disparate amounts of P-TnI intensities resulted in variable yellow intensities on the merged picture of the HF pacing group. **b** Capturing images of P-TnI stained slices under a confocal microscope revealed cell-to-cell differences: clusters of cardiomyocytes with divergent levels of TnI phosphorylation could be distinguished in the HF animals at the pacing site

contrast with the histogram of the HF pacing site, which appeared to be asymmetrical due to an increase in cardiomyocyte count at relatively low [log(P-TnI/TnI)] ratios. In agreement with the results of our back-phosphorylation assays (Fig. 2a, b), the mean value of [log(P-TnI/TnI)] at the HF pacing site was significantly lower than that at the

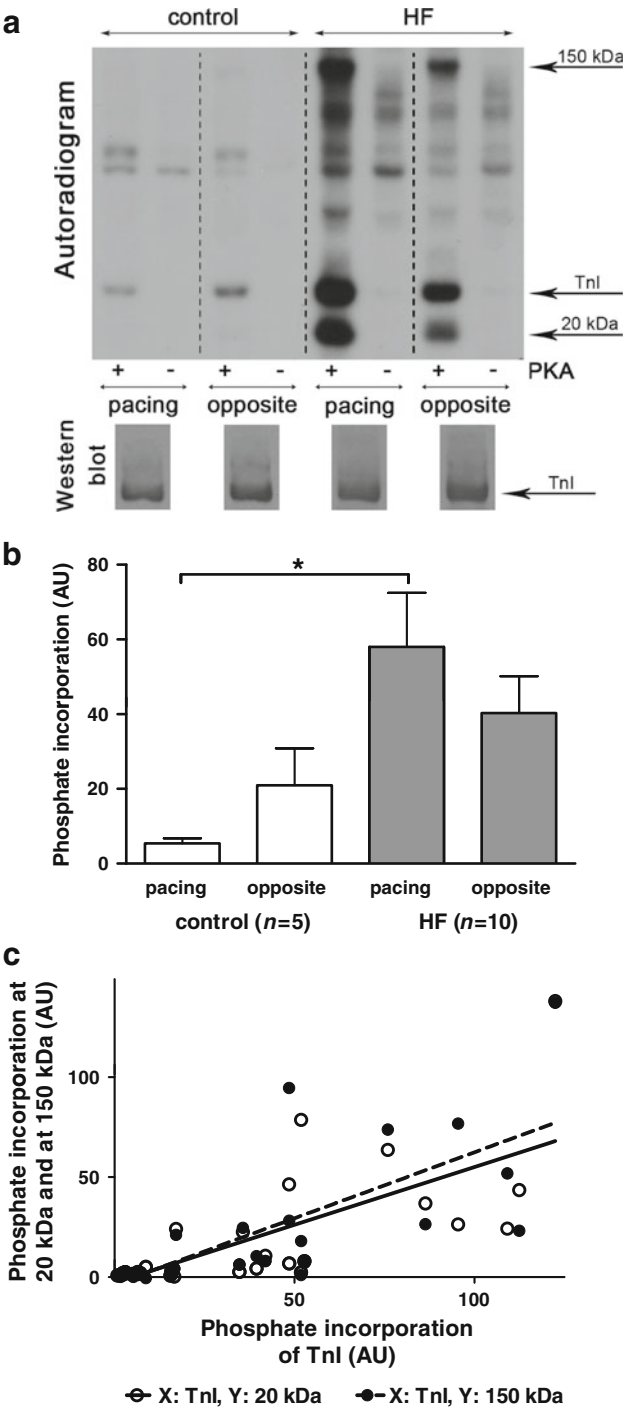


**Fig. 2** TnI back-phosphorylation. **a** Results of autoradiography (*top*) and western immunoblotting (*bottom*) in a representative TnI back-phosphorylation assay. $^{32}$P-labeled ATP was used to determine PKA-dependent phosphate incorporation into TnI at the pacing and opposite LV sites in control and HF animals following SDS gel electrophoresis. Signal intensities in the autoradiograms were considered to be directly proportional to the extents of inorganic phosphate ($P_i$) incorporation into TnI in the presence of PKA (+ signs) in vitro, and inversely proportional to the initial levels of phosphorylation of TnI prior to PKA application in vivo. Signal intensities in the absence of PKA were negligible (− signs). Western immunoblots developed with a TnI-sensitive antibody confirmed comparable protein loads during all tests. **b** Statistical analysis on the results of back-phosphorylation assays under identical conditions suggested a lower mean level of TnI phosphorylation for the HF pacing site than for the control pacing site (columns show means ± SEM; *n* number of animals, AU optical density in arbitrary units, $*P < 0.05$ HF pacing vs. control pacing site). **c** Correlations between TnI phosphorylation and additional proteins at 20 and 150 kDa. Signal intensities at 20 and 150 kDa from pacing and opposite sites of individual animals were plotted in an *X*–*Y* diagram as functions of $P_i$ incorporation into TnI in the respective samples. *Lines* represent relationships between phosphorylation at 20 or 150 kDa and TnI phosphorylation from linear regression analyses, suggesting positive correlations between these variables ($r = 0.71$, $P < 0.0001$; $r = 0.74$, $P < 0.0001$, respectively)

same site in the control animals (−0.41 vs. −0.28 for the HF pacing site and the control pacing site, respectively; $P = 0.0071$), and hence both of these assays pointed to a relative reduction in P-TnI in the paced region of failing hearts. Moreover, the IQR in this group was significantly higher than that at the pacing site of the controls or at the opposite site of failing hearts (0.53 vs. 0.36 or 0.42, for the HF pacing, control pacing and HF opposite sites, respectively; $P = 0.0093$ vs. control pacing site; $P = 0.0047$ vs. HF opposite site). The widening of the IQR at the HF pacing site reflected the increased scatter in the levels of relative TnI phosphorylation at the pacing site among the cardiomyocytes of failing hearts. Descriptive values of distribution histograms are given in Table 1.

Mean levels of log(P-TnI/TnI) intensities with 95% confidence intervals for each animal are illustrated in Fig. 4. This representation allowed us to analyze the variability of TnI phosphorylation in the different regions of interest in the individual control and failing hearts. In general, the log(P-TnI/TnI) values for the control hearts were scattered in a narrower range than those for the failing hearts. Further, in the control animals the means of log(P-TnI/TnI) were randomly higher or lower for the pacing or opposite sites, and the differences between these two sites (with the exception of control 4) were small. In contrast, in HF (with the exception of HF 6) the means for the log(P-TnI/TnI) values at the pacing sites were lower than those at the opposite sites. Moreover, the differences between the two sites of individual failing hearts were about twice the mean difference detected within the control group.

A hypothetical difference in cardiomyocyte mechanics was also studied by means of direct force measurements on single permeabilized cardiomyocytes isolated from HF and control animals (Fig. 5). $Ca^{2+}$ sensitivity curves of isometric force production ($Ca^{2+}$–force relations) were determined for individual cardiomyocytes and subsequently averaged in all groups at 2.3 μm SL before and after PKA exposures (Fig. 5a–d). Force values at intermediate [$Ca^{2+}$] were normalized to maximal $Ca^{2+}$-activated force ($F_o$) and

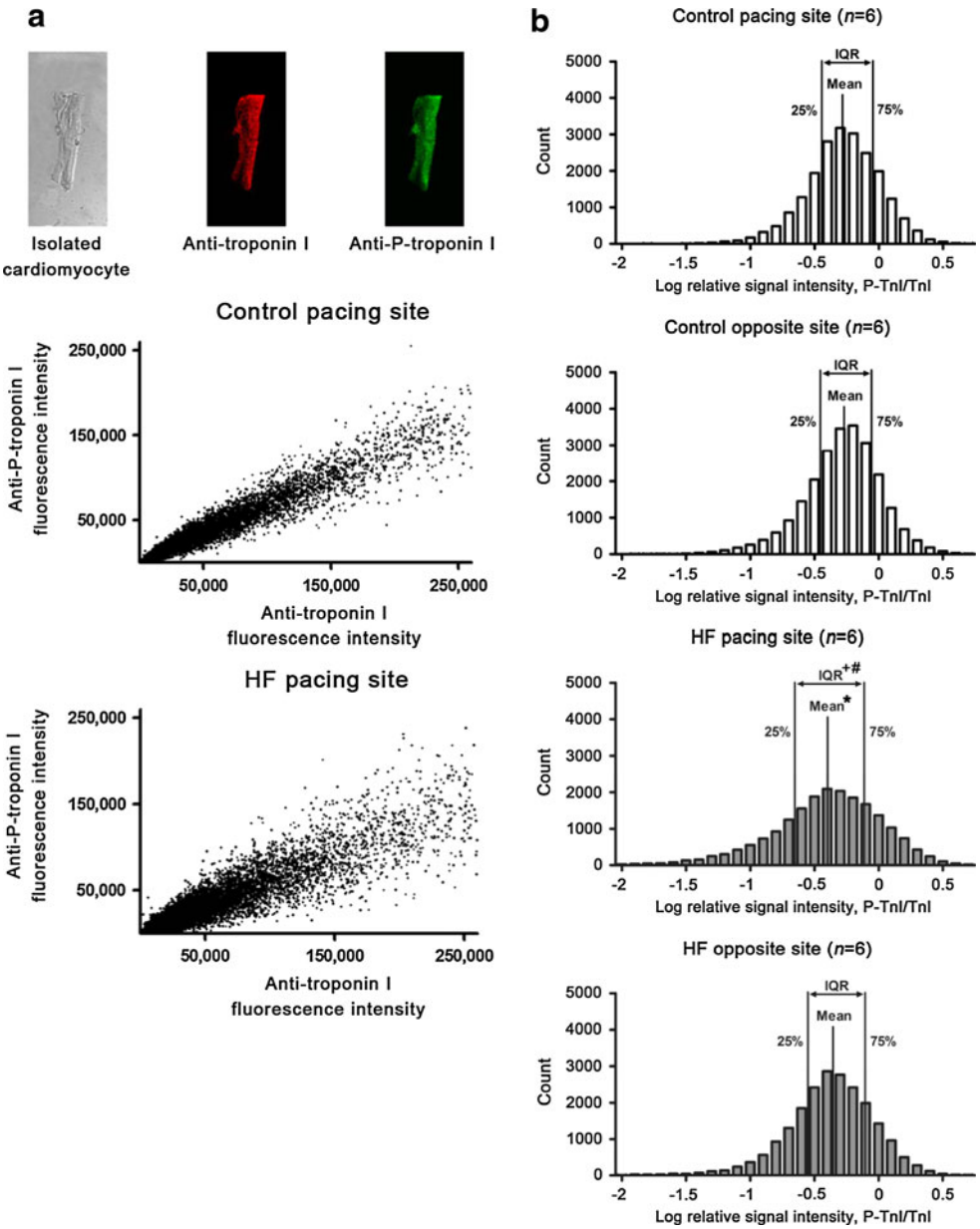


**Fig. 3** Flow cytometry. **a** Microscopic images of a representative permeabilized cardiomyocyte (*top panel*) dual-labeled for TnI (*red*) and P-TnI (*green*) for flow cytometric evaluation. Signal intensities were plotted in *X–Y* diagrams, where the values on the *X* and *Y* axes reflected TnI and P-TnI intensity levels, respectively (*middle* and *lower panels*, $n \approx 20{,}000$ cardiomyocytes from 6 hearts). The wider scatter of the data obtained from the HF pacing site (*bottom panel*) than those from the control pacing site (*middle panel*) suggested more heterogeneous TnI phosphorylation levels in the cardiomyocytes of the HF animals in the paced area. **b** Distribution of relative TnI phosphorylation in isolated cardiomyocytes. Distribution profiles of logarithmically transformed relative signal intensities [log(P-TnI/TnI)] were expressed for the four groups. (The IQRs between the 25 and 75 percentile values of the distribution histograms are highlighted; *n* number of animals; $^{*}P = 0.0071$ HF pacing vs. control pacing site; $^{+}P = 0.0093$ HF pacing vs. control pacing site; $^{\#}P = 0.0047$ HF pacing vs. HF opposite site)

plotted as a function of pCa. A Hill function was then used to determine $pCa_{50}$, which therefore illustrated the $Ca^{2+}$ sensitivity of force production. Mean $pCa_{50}$ values of control hearts at the pacing site did not differ significantly from those of the opposite site in control and HF hearts before PKA treatments ($5.77 \pm 0.01$, $5.75 \pm 0.01$ and $5.73 \pm 0.03$, respectively). However, mean $pCa_{50}$ (and hence $Ca^{2+}$ sensitivity of force production) was significantly higher at the pacing site of HF hearts ($5.86 \pm 0.03$) than at all the other sites of HF and control hearts. Moreover, PKA exposures reduced $pCa_{50}$ by the largest degree in cardiomyocytes of the pacing site of HF animals, thereby eliminating the differences in the $Ca^{2+}$ sensitivities of force production among the four groups of cardiomyocytes. In addition, the distributions of $pCa_{50}$ at the pacing sites of the failing and the control hearts resembled the characteristics of those obtained in our flow cytometric assays and were therefore also in agreement with the biochemical and histochemical findings (Fig. 5e–h). Furthermore, in vitro PKA treatments evoked a wider range in $Ca^{2+}$ sensitivity reductions at the HF pacing site than at all other sites. Mean values of $F_o$, $F_{passive}$ and the cross-bridge-sensitive $k_{tr,max}$ are given in Table 2. $F_{passive}$ at the HF pacing site was significantly higher than at the HF opposite site; however, no significant differences in $F_o$ and in maximal actin-myosin cross-bridge cycle rates ($k_{tr,max}$) were found between the different experimental groups.

In a separate study, the length dependencies of the mechanical parameters were investigated by performing force measurements at the SL of 1.9 μm and subsequently

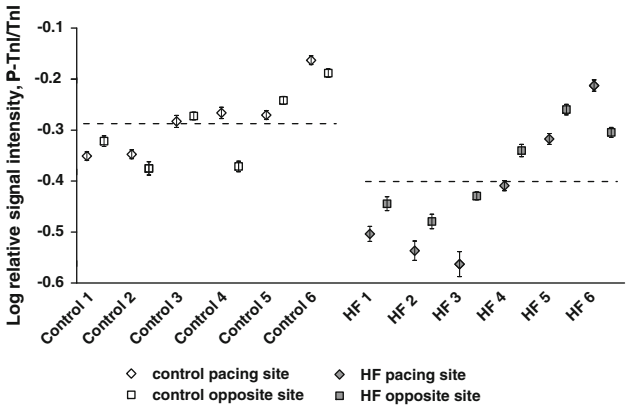


**Fig. 4** TnI phosphorylation in experimental animals. Mean levels of [log(P-TnI/TnI)] intensities with 95% confidence intervals for each site of each animal. *Horizontal lines* indicate average [log(P-TnI/TnI)] values of control and HF pacing sites. The [log(P-TnI/TnI)] values for the control animals were scattered in a narrower range than those for the HF animals

at the SL of 2.3 μm. In short, length dependencies of $F_o$, $F_{passive}$, and the $Ca^{2+}$ sensitivity of force production were observed in all groups of cardiomyocytes, implying that the stretch-dependent mechanical characteristics of the cardiomyocytes are well preserved during the development of pacing-induced HF (data not shown).

## Discussion

The results of this study have revealed a non-uniform down-regulation of myocardial PKA-dependent TnI phosphorylation in a porcine model of pacing-induced HF. Interestingly, the cell-to-cell variability in the level of P-TnI was larger in the vicinity of the pacing electrode than in non-paced regions of the LV. Consequently, we propose that the inhomogeneity in PKA-dependent contractile protein hypophosphorylation may contribute to the regional mechanical dysfunction of the remodeled myocardium in this model of HF.

Dyssynchrony in ventricular contractile responses is considered to be a major contributor of the mechanical dysfunction in the remodeled LV, and hence electrical resynchronization offers benefit for HF patients with a significant QRS prolongation [32]. Regional myocardial differences have repeatedly been noted in various models of HF induced by electrical stimulation [10, 14, 23, 25, 38]. In open-chest anesthetized dogs, abnormal wall motion at the target site of the LV yielded early shortening and late systolic lengthening, whereas the shortening pattern at the remote site remained unaffected [14]. Various mechanisms have been postulated to explain these region-specific changes, ranging from matrix metalloproteinase-9 activation [14] to transmural and trans-chamber expression gradients of proteins such as phosphorylated ERK mitogen-activated protein kinase, sarcoplasmic reticulum $Ca^{2+}$-ATPase, phospholamban, or gap junction protein connexin 43 [20, 38]. Paracrine/autocrine signaling mechanisms have also been stressed as players in the development of regional tissue alterations in pacing-induced HF. For instance, the cardiotropin-1 expression was found to be preferably increased in the vicinity of the pacemaker [31]. In a canine model of pacing-induced HF, an orchestrated shift in the pattern of expression of respiratory chain subunits, mitochondrial bioenergetic enzymes, and apoptotic proteins with distinct differences in the regional distribution and in the subpopulations of mitochondria have been described [25]. Collectively, it is currently not entirely clear which signaling processes are primarily involved in regional mechanical alterations and how they are linked with potential changes in the $Ca^{2+}$ responsiveness of the myofilaments and/or with the $Ca^{2+}$ handling of cardiomyocytes [1, 2, 17]. Nevertheless, it is tempting to speculate that paracrine responses to natriuretic peptides may relate to interactions between cGMP and cAMP-dependent intracellular signaling [13].

In view of the central position of the $\beta$-adrenergic cascade in the regulation of myocardial contractility, several previous investigations addressed its hypothetical involvement in the regional characteristics of pacing-induced HF. Indeed, the efferent sympathetic function and $\beta$-adrenergic responsiveness appeared to be reduced in association with the development of pacing-induced HF in dogs with region-specific alterations in function [19, 36], although the biochemical and cellular parameters of $\beta$-adrenergic signaling did not clearly exhibit regional characteristics [3, 18, 36,

**Table 2** Mean values of active, passive force and $k_{tr,max}$ obtained during direct force measurements in permeabilized cardiomyocytes

| | Control pacing site ($n = 23$) | Control opposite site ($n = 20$) | HF pacing site ($n = 21$) | HF opposite site ($n = 29$) |
|---|---|---|---|---|
| $F_o$ (kN/m$^2$) | 12.83 ± 1.73 | 15.47 ± 1.84 | 12.05 ± 1.15 | 16.81 ± 1.42 |
| $F_{passive}$ (kN/m$^2$) | 1.46 ± 0.20 | 1.69 ± 0.43 | 2.26 ± 0.48* | 1.17 ± 0.11 |
| $k_{tr,max}$ (1/s) | 0.81 ± 0.06 | 0.75 ± 0.04 | 0.82 ± 0.05 | 0.96 ± 0.05 |

Values are means ± SEM

*n* number of cardiomyocytes from 5 control and 8 HF hearts

* $P < 0.05$ HF pacing versus HF opposite site

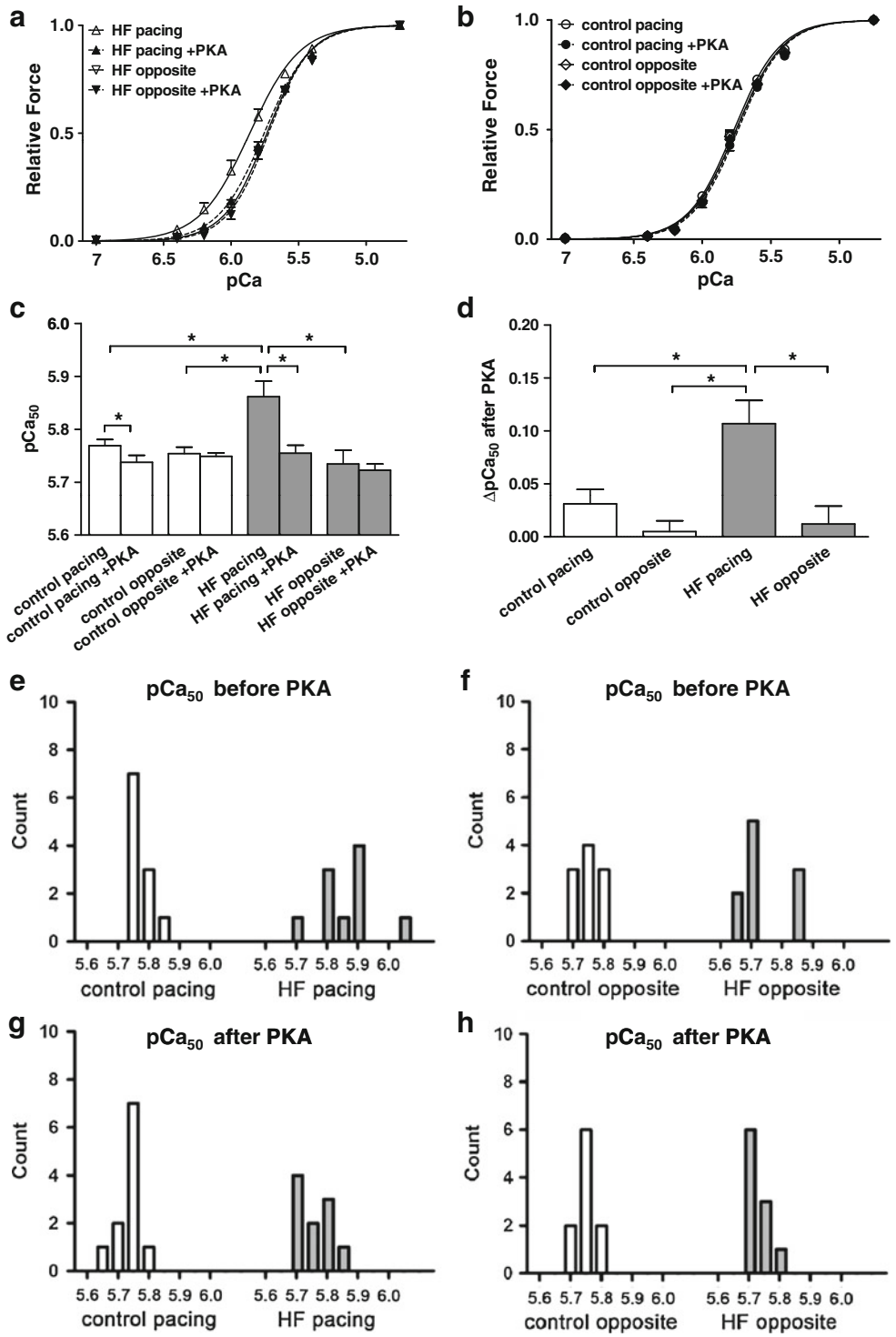


40]. At the cardiomyocyte level, a decrease in basal $\beta$-adrenergic signaling would predict an increase in the $Ca^{2+}$ sensitivity of myofibrillar force production, a change often correlated with the coordinated hypophosphorylation of TnI and MyBP-C [21, 24, 43]. Experimental data obtained during an in situ assessment of myofilament $Ca^{2+}$ responsiveness suggested either preserved or decreased $Ca^{2+}$ sensitivity of myofibrillar force production in a canine model of pacing-induced HF [16]. Moreover, in the porcine model of pacing-induced HF, the relative increase in LV contractility in response to low-dose dobutamine stimulation was higher at the pacing site than at the opposite site, although the basal contractility was lower at the pacing site than at the opposite site [22].

◀ **Fig. 5** Mean $Ca^{2+}$–force relations and distributions of $pCa_{50}$ values in isolated cardiomyocytes. **a** $Ca^{2+}$–force relations of isolated cardiomyocytes obtained from the pacing and opposite sites of the HF animals before and after in vitro PKA treatments. The leftward position of the $Ca^{2+}$–force relations at the HF pacing site before PKA treatment illustrated an increased $Ca^{2+}$-sensitivity of force production in cardiomyocytes of this region relative to all others. After PKA treatment, a rightward shift in the $Ca^{2+}$–force relation was observed. **b** Small differences between the $Ca^{2+}$–force relationships of the control pacing and control opposite groups could be detected before and after in vitro PKA treatment. **c** Means of $pCa_{50}$ values in the four groups of cardiomyocytes before and after in vitro PKA treatment. Mean $pCa_{50}$ at the HF pacing site was significantly higher than in all other groups under basal conditions, and this difference could be eliminated by PKA ($*P < 0.05$). **d** PKA-evoked changes in $pCa_{50}$ values in the four experimental groups. The effect of PKA on mean $pCa_{50}$ was the highest at the pacing site of HF animals ($*P < 0.05$). The Hill coefficient did not differ significantly among the four experimental groups before and after PKA exposures ($n_{Hill} \sim 2.6$). **e–h** Distributions of $pCa_{50}$ values in cardiomyocytes from the four experimental groups before and after in vitro PKA treatment. $pCa_{50}$ values of the HF pacing group were dispersed on a wider range than in all other groups. After PKA treatment, a narrower distribution for the $pCa_{50}$ values could be measured in HF cardiomyocytes at the pacing site

In our present study, we focused not only on regional, but also on intraregional aspects of a hypothetically blunted PKA-mediated TnI phosphorylation, along with the development of pacing-induced HF in pigs. We hypothesized that tissue-level alterations in TnI phosphorylation driven by the $\beta$-adrenergic system might be associated with regional differences in the mechanical function of the remodeled myocardium. Our back-phosphorylation assays revealed significantly decreased TnI phosphorylation at the pacing site of the HF animals as compared with the controls, consistently with a hypothetical down-regulation of the $\beta$-adrenergic system at the pacing site of the HF animals and hence implying an increase in the $Ca^{2+}$ sensitivity of myofibrillar force production ($pCa_{50}$). Accordingly, the mean $pCa_{50}$ values were significantly higher at the HF pacing site than at the opposite site or both sides in controls, and this difference could be eliminated by in vitro PKA treatments. In addition, immunohistochemistry, flow cytometry, and direct force measurements confirmed a relatively high cell-to-cell variability in the relative P-TnI levels at the pacing site of the HF animals. The preservation of most of the mechanical parameters in the cardiomyocytes of the paced region of the HF animals (e.g. the SL dependence of the $Ca^{2+}$ sensitivity of force production, $k_{tr,max}$, etc.) suggested an unchanged Frank-Starling mechanism and cross-bridge cycling rates in these cardiomyocytes. Overall, our observations suggested that alterations in the myofilament function of the cardiomyocytes were mirrored by $pCa_{50}$ at the pacing site of the HF animals, a change that can be correlated to PKA-dependent TnI and MyBP-C phosphorylation. Therefore, we propose that dysregulation of PKA-dependent contractile protein phosphorylation may contribute to the regional contractile dysfunction observed in the porcine model of pacing-induced HF [23]. Additionally, the increase in $F_{passive}$ at the pacing site due to PKA-dependent hypophosphorylation of other myofilament proteins (e.g. titin) could participate in the increase in LV end-diastolic pressure in these hearts (from $\sim$6 to $\sim$ 20 mmHg) [7]. Nevertheless, our present investigations did not clarify to which extent regional alterations in myofilament protein phosphorylation were involved in functional hemodynamic alterations (e.g. reduction in the ejection fraction from $\sim$76 to $\sim$35%) [23].

To the best of our knowledge, this is the first analysis of tissue-level inhomogeneities in cardiomyocyte TnI phosphorylation through a combination of a number of sensitive methods (protein biochemistry, histochemistry, direct force measurements and cell cytometry) during the development of non-ischemic HF. A diminishing transmural gradient in contractile protein phosphorylation has previously been implicated in post-ischemic myocardial remodeling in rats [9], although similar features have not been demonstrated in dogs suffering from pacing-induced HF [20]. Our data revealed that the level of TnI phosphorylation spans a wider range in the vicinity of the pacing electrode than elsewhere and suggested that it can be distinctly different in clusters of cardiomyocytes during pacing-induced HF. At present, we cannot provide an explanation for this distribution pattern of P-TnI staining intensity; we speculate that it may be related to the physical characteristics of the stimulating electrical current on the myocardium.

Overall, the rapid pacing of the LV induced the remodeling of porcine hearts and led to HF, which could be characterized by an overall decrease in PKA-mediated TnI phosphorylation close to the site of electrical stimulation. The level of PKA-dependent phosphorylation of TnI exhibited a larger cell-to-cell variation in the paced region of the LV than in more remote areas or in controls. This intraregional inhomogeneity in this $\beta$-adrenergic-dependent variable affects the $Ca^{2+}$ sensitivity of myofibrillar force production and may thereby contribute to dyssynchronous and hence impaired LV contractions in the porcine model of pacing-induced HF.

**Acknowledgments** The authors are grateful to Dr. László Kardos for support with the statistical analyses. The work was supported by the TÁMOP 4.2.1./B-09/1/KONV-2010-0007 project and OTKA grant K 68363 and by the European Union Project FP7-HEALTH-2010: ''MEDIA-Metabolic Road to Diastolic Heart Failure'' MEDIA-261409. The project is implemented through the New Hungary Development Plan, co-financed by the European Social Fund.

## References


1. Aiba T, Hesketh GG, Barth AS, Liu T, Daya S, Chakir K, Dimaano VL, Abraham TP, O'Rourke B, Akar FG, Kass DA, Tomaselli GF (2009) Electrophysiological consequences of dyssynchronous heart failure and its restoration by resynchronization therapy. Circulation 119:1220–1230. doi:10.1161/CIRCULATIONAHA.108.794834
2. Aiba T, Tomaselli GF (2010) Electrical remodeling in the failing heart. Curr Opin Cardiol 25:29–36. doi:10.1097/HCO.0b013e328333d3d6
3. Anzai T, Lai NC, Gao M, Hammond HK (1998) Dissociation between regional dysfunction and beta-adrenergic receptor signaling in heart failure. Am J Physiol 275:H1267–H1273
4. Belin RJ, Sumandea MP, Allen EJ, Schoenfelt K, Wang H, Solaro RJ, de Tombe PP (2007) Augmented protein kinase C-alpha-induced myofilament protein phosphorylation contributes to myofilament dysfunction in experimental congestive heart failure. Circ Res 101:195–204. doi:10.1161/CIRCRESAHA.107.148288
5. Belin RJ, Sumandea MP, Kobayashi T, Walker LA, Rundell VL, Urboniene D, Yuzhakova M, Ruch SH, Geenen DL, Solaro RJ, de Tombe PP (2006) Left ventricular myofilament dysfunction in rat experimental hypertrophy and congestive heart failure. Am J Physiol Heart Circ Physiol 291:H2344–H2353. doi:10.1152/ajpheart.00541.2006
6. Bodor GS, Oakeley AE, Allen PD, Crimmins DL, Ladenson JH, Anderson PA (1997) Troponin I phosphorylation in the normal and failing adult human heart. Circulation 96:1495–1500. doi:10.1161/01.CIR.96.5.1495
7. Borbely A, Falcao-Pires I, van Heerebeek L, Hamdani N, Edes I, Gavina C, Leite-Moreira AF, Bronzwaer JG, Papp Z, van der Velden J, Stienen GJ, Paulus WJ (2009) Hypophosphorylation of the Stiff N2B titin isoform raises cardiomyocyte resting tension in failing human myocardium. Circ Res 104:780–786. doi:10.1161/circresaha.108.193326
8. Borbely A, Toth A, Edes I, Virag L, Papp JG, Varro A, Paulus WJ, van der Velden J, Stienen GJ, Papp Z (2005) Peroxynitrite-induced alpha-actinin nitration and contractile alterations in isolated human myocardial cells. Cardiovasc Res 67:225–233. doi:10.1016/j.cardiores.2005.03.025
9. Cazorla O, Szilagyi S, Le Guennec JY, Vassort G, Lacampagne A (2005) Transmural stretch-dependent regulation of contractile properties in rat heart and its alteration after myocardial infarction. FASEB J 19:88–90. doi:10.1096/fj.04-2066fje
10. Del Ry S, Cabiati M, Lionetti V, Simioniuc A, Caselli C, Prescimone T, Emdin M, Giannessi D (2009) Asymmetrical myocardial expression of natriuretic peptides in pacing-induced heart failure. Peptides 30:1710–1713. doi:10.1016/j.peptides.2009.06.013
11. Edes IF, Toth A, Csanyi G, Lomnicka M, Chlopicki S, Edes I, Papp Z (2008) Late-stage alterations in myofibrillar contractile function in a transgenic mouse model of dilated cardiomyopathy (Tgalphaq*44). J Mol Cell Cardiol 45:363–372. doi:10.1016/j.yjmcc.2008.07.001
12. Falcao-Pires I, Palladini G, Goncalves N, van der Velden J, Moreira-Goncalves D, Miranda-Silva D, Salinaro F, Paulus WJ, Niessen HW, Perlini S, Leite-Moreira AF (2011) Distinct mechanisms for diastolic dysfunction in diabetes mellitus and chronic pressure-overload. Basic Res Cardiol 106:801–814. doi:10.1007/s00395-011-0184-x
13. Fischmeister R, Castro LR, Abi-Gerges A, Rochais F, Jurevicius J, Leroy J, Vandecasteele G (2006) Compartmentation of cyclic nucleotide signaling in the heart: the role of cyclic nucleotide phosphodiesterases. Circ Res 99:816–828. doi:10.1161/01.RES.0000246118.98832.04
14. Garcia RA, Brown KL, Pavelec RS, Go KV, Covell JW, Villarreal FJ (2005) Abnormal cardiac wall motion and early matrix metalloproteinase activity. Am J Physiol Heart Circ Physiol 288:H1080–H1087. doi:10.1152/ajpheart.00860.2004
15. Heusch G (2011) Heart rate and heart failure. Not a simple relationship. Circ J 75:229–236. doi:10.1253/circj.CJ-10-0925
16. Heusch G, Neumann T (1998) Calcium responsiveness in canine pacing-induced heart failure. J Mol Cell Cardiol 30:1605–1613. doi:10.1006/jmcc.1998.0726
17. Heusch G, Rose J, Skyschally A, Post H, Schulz R (1996) Calcium responsiveness in regional myocardial short-term hibernation and stunning in the in situ porcine heart. Inotropic responses to postextrasystolic potentiation and intracoronary calcium. Circulation 93:1556–1566. doi:10.1161/01.CIR.93.8.1556
18. Hinton RB, Hebbar L, Cox MH, Mukherjee R, Joshi JD, Crawford FA Jr, Spinale FG (1997) Left ventricular regional myocyte contractility in normal and heart failure states. J Mol Cell Cardiol 29:1939–1946. doi:10.1006/jmcc.1997.0434
19. Huang MW, Leone RJ Jr, Weiss HR, Tse J, Scholz PM (2000) Effects of beta-adrenoceptor stimulation on pacing-induced failure of dog hypertrophic hearts. Clin Exp Pharmacol Physiol 27:202–207. doi:10.1046/j.1440-1681.2000.03229.x
20. Igarashi-Saito K, Tsutsui H, Takahashi M, Kinugawa S, Egashira K, Takeshita A (1999) Endocardial versus epicardial differences of sarcoplasmic reticulum $Ca^{2+}$-ATPase gene expression in the canine failing myocardium. Basic Res Cardiol 94:267–273. doi:10.1007/s003950050152
21. Kooij V, Boontje N, Zaremba R, Jaquet K, dos Remedios C, Stienen GJ, van der Velden J (2010) Protein kinase C alpha and epsilon phosphorylation of troponin and myosin binding protein C reduce $Ca^{2+}$ sensitivity in human myocardium. Basic Res Cardiol 105:289–300. doi:10.1007/s00395-009-0053-z
22. Lionetti V, Aquaro GD, Simioniuc A, Di Cristofano C, Forini F, Cecchetti F, Campan M, De Marchi D, Bernini F, Grana M, Nannipieri M, Mancini M, Lombardi M, Recchia FA, Pingitore A (2009) Severe mechanical dyssynchrony causes regional hibernation-like changes in pigs with nonischemic heart failure. J Card Fail 15:920–928. doi:10.1016/j.cardfail.2009.06.436
23. Lionetti V, Guiducci L, Simioniuc A, Aquaro GD, Simi C, De Marchi D, Burchielli S, Pratali L, Piacenti M, Lombardi M, Salvadori P, Pingitore A, Neglia D, Recchia FA (2007) Mismatch between uniform increase in cardiac glucose uptake and regional contractile dysfunction in pacing-induced heart failure. Am J Physiol Heart Circ Physiol 293:H2747–H2756. doi:10.1152/ajpheart.00592.2007
24. Luss H, Meissner A, Rolf N, Van Aken H, Boknik P, Kirchhefer U, Knapp J, Laer S, Linck B, Luss I, Muller FU, Neumann J, Schmitz W (2000) Biochemical mechanism(s) of stunning in conscious dogs. Am J Physiol Heart Circ Physiol 279:H176–H184
25. Marin-Garcia J, Goldenthal MJ, Damle S, Pi Y, Moe GW (2009) Regional distribution of mitochondrial dysfunction and apoptotic remodeling in pacing-induced heart failure. J Card Fail 15:700–708. doi:10.1016/j.cardfail.2009.04.010
26. Marston SB, de Tombe PP (2008) Troponin phosphorylation and myofilament $Ca^{2+}$-sensitivity in heart failure: increased or decreased? J Mol Cell Cardiol 45:603–607. doi:10.1016/j.yjmcc.2008.07.004
27. Messer AE, Jacques AM, Marston SB (2007) Troponin phosphorylation and regulatory function in human heart muscle: dephosphorylation of Ser23/24 on troponin I could account for the contractile defect in end-stage heart failure. J Mol Cell Cardiol 42:247–259. doi:10.1016/j.yjmcc.2006.08.017
28. Montgomery DE, Rundell VL, Goldspink PH, Urboniene D, Geenen DL, de Tombe PP, Buttrick PM (2005) Protein kinase C epsilon induces systolic cardiac failure marked by exhausted inotropic reserve and intact Frank-Starling mechanism. Am J Physiol Heart Circ Physiol 289:H1881–H1888. doi:10.1152/ajpheart.00454.2005

29. Papp Z, Szabo A, Barends JP, Stienen GJ (2002) The mechanism of the force enhancement by MgADP under simulated ischaemic conditions in rat cardiac myocytes. J Physiol 543:177–189. doi:10.1113/jphysiol.2002.022145
30. Perez NG, Hashimoto K, McCune S, Altschuld RA, Marban E (1999) Origin of contractile dysfunction in heart failure: calcium cycling versus myofilaments. Circulation 99:1077–1083
31. Potter DD, Araoz PA, Ng LL, Kruger DG, Thompson JL 3rd, Hamner CE, Rysavy JA, Mandrekar JN, Sundt TM 3rd (2007) Cardiotropin-1 and myocardial strain change heterogeneously in cardiomyopathy. J Surg Res 141:277–283. doi:10.1016/j.jss.2006.12.539
32. Prinzen FW, Peschar M (2002) Relation between the pacing induced sequence of activation and left ventricular pump function in animals. Pacing Clin Electrophysiol 25:484–498. doi:10.1046/j.1460-9592.2002.00484.x
33. Purcell IF, Bing W, Marston SB (1999) Functional analysis of human cardiac troponin by the in vitro motility assay: comparison of adult, foetal and failing hearts. Cardiovasc Res 43:884–891. doi:10.1016/S0008-6363(99)00123-6
34. Recchia FA, Lionetti V (2007) Animal models of dilated cardiomyopathy for translational research. Vet Res Commun 31(Suppl 1):35–41. doi:10.1007/s11259-007-0005-8
35. Richter W, Xie M, Scheitrum C, Krall J, Movsesian MA, Conti M (2011) Conserved expression and functions of PDE4 in rodent and human heart. Basic Res Cardiol 106:249–262. doi:10.1007/s00395-010-0138-8
36. Simmons WW, Freeman MR, Grima EA, Hsia TW, Armstrong PW (1994) Abnormalities of cardiac sympathetic function in pacing-induced heart failure as assessed by [123I]metaiodobenzylguanidine scintigraphy. Circulation 89:2843–2851
37. Skyschally A, Gres P, van Caster P, van de Sand A, Boengler K, Schulz R, Heusch G (2008) Reduced calcium responsiveness characterizes contractile dysfunction following coronary microembolization. Basic Res Cardiol 103:552–559. doi:10.1007/s00395-008-0732-1
38. Spragg DD, Leclercq C, Loghmani M, Faris OP, Tunin RS, DiSilvestre D, McVeigh ER, Tomaselli GF, Kass DA (2003) Regional alterations in protein expression in the dyssynchronous failing heart. Circulation 108:929–932. doi:10.1161/01.CIR.0000088782.99568.CA
39. Szentesi G, Horvath G, Bori I, Vamosi G, Szollosi J, Gaspar R, Damjanovich S, Jenei A, Matyus L (2004) Computer program for determining fluorescence resonance energy transfer efficiency from flow cytometric data on a cell-by-cell basis. Comput Methods Programs Biomed 75:201–211. doi:10.1016/j.cmpb.2004.02.004
40. Takahama H, Asanuma H, Sanada S, Fujita M, Sasaki H, Wakeno M, Kim J, Asakura M, Takashima S, Minamino T, Komamura K, Sugimachi M, Kitakaze M (2010) A histamine H receptor blocker ameliorates development of heart failure in dogs independently of beta-adrenergic receptor blockade. Basic Res Cardiol 105:787–794. doi:10.1007/s00395-010-0119-y
41. van der Velden J, Boontje NM, Papp Z, Klein LJ, Visser FC, de Jong JW, Owen VJ, Burton PB, Stienen GJ (2002) Calcium sensitivity of force in human ventricular cardiomyocytes from donor and failing hearts. Basic Res Cardiol 97(Suppl 1):I118–I126. doi:10.1007/s003950200040
42. van der Velden J, Klein LJ, Zaremba R, Boontje NM, Huybregts MA, Stooker W, Eijsman L, de Jong JW, Visser CA, Visser FC, Stienen GJ (2001) Effects of calcium, inorganic phosphate, and pH on isometric force in single skinned cardiomyocytes from donor and failing human hearts. Circulation 104:1140–1146. doi:10.1161/hc3501.095485
43. van der Velden J, Papp Z, Zaremba R, Boontje NM, de Jong JW, Owen VJ, Burton PB, Goldmann P, Jaquet K, Stienen GJ (2003) Increased $Ca^{2+}$-sensitivity of the contractile apparatus in end-stage human heart failure results from altered phosphorylation of contractile proteins. Cardiovasc Res 57:37–47. doi:10.1016/S0008-6363(02)00606-5
44. Verduyn SC, Zaremba R, van der Velden J, Stienen GJ (2007) Effects of contractile protein phosphorylation on force development in permeabilized rat cardiac myocytes. Basic Res Cardiol 102:476–487. doi:10.1007/s00395-007-0663-2
45. Wolff MR, Buck SH, Stoker SW, Greaser ML, Mentzer RM (1996) Myofibrillar calcium sensitivity of isometric tension is increased in human dilated cardiomyopathies: role of altered beta-adrenergically mediated protein phosphorylation. J Clin Invest 98:167–176. doi:10.1172/JCI118762